Chinese Chemical Letters 33 (2022) 2496–2500

Contents lists available at ScienceDirect

Chinese Chemical Letters

journal homepage: www.elsevier.com/locate/cclet

Targeting the Rac1 pathway for improved prostate cancer therapy using polymeric nanoparticles to deliver of NSC23766

Zean Li[a,c,d,1], Jun Huang[b,1], Tao Du[e,1], Yiming Lai[a,c], Kaiwen Li[a,c], Man-Li Luo[c,d], Dingjun Zhu[a,c,d,*], Jun Wu[b,**], Hai Huang[a,c,d,f,*]

[a] Department of Urology, Sun Yat-sen Memorial Hospital, Sun Yat-sen University, Guangzhou 510220, China
[b] School of Biomedical Engineering, Sun Yat-sen University, Shenzhen 518107, China
[c] Guangdong Provincial Key Laboratory of Malignant Tumor Epigenetics and Gene Regulation, Sun Yat-sen Memorial Hospital, Sun Yat-sen University, Guangzhou 510120, China
[d] Medical Research Center, Sun Yat-sen Memorial Hospital, Sun Yat-sen University, Guangzhou 510120, China
[e] Department of Obstetrics and Gynecology, Sun Yat-sen Memorial Hospital, Sun Yat-sen University, Guangzhou 510120, China
[f] Department of Urology, The Sixth Affiliated Hospital of Guangzhou Medical University, Qingyuan People's Hospital, Qingyuan 511518, China

ARTICLE INFO

Article history:
Received 14 September 2021
Revised 23 November 2021
Accepted 26 November 2021
Available online 2 December 2021

Keywords:
Prostate cancer
NSC23766
Rac1
Nanoparticle
Poly(ester amide)

ABSTRACT

Prostate cancer (PCa) is the second most commonly diagnosed cancer in men. The Rac1-GTP inhibitor NSC23766 has been shown to suppress PCa growth. However, these therapies have low tumor-targeting efficacy *in vivo*. Therefore, it is essential to produce a drug delivery system that specifically targets the tumor site. Herein, novel L-phenylalanine-based poly(ester amide) (Phe-PEA) polymers were synthesized and loaded with NSC23766 (NSC23766@8P6 NPs), which had a small particle size (162.3 ± 6.7 nm) and high NSC23766 loading ($8.0\% \pm 1.1\%$) with a more rapid release of NSC23766 at pH 5.0. *In vitro* cellular uptake and cytotoxicity assays demonstrated that NSC23766@8P6 NPs were rapidly taken up by PC3 cells and showed significant effects of PCa cell proliferation inhibition and G2/M phase arrest. Furthermore, *in vivo* studies using PC3-bearing mice demonstrated that NSC23766@8P6 NPs delivered by intravenous injection not only increased the drug concentration with prolonged retention (96 h) at the tumor site, but also inhibited tumor growth and induced apoptosis. In conclusion, we have discovered that NSC23766@8P6 NPs can serve as a delivery system that targets the tumor site and is therefore a promising therapeutic approach for PCa treatment.

Prostate cancer (PCa) is the second most frequent cancer in men, accounting for 13.5% of all malignant tumor cases in the world [1–3]. After 2–3 years of remission, most PCa patients will develop resistance to traditional therapy [4,5]. Therefore, there is an urgent need to improve the efficiency of traditional therapies and discover novel therapeutic targets for PCa. Several crucial signaling pathways that contribute to the progression of PCa, such as the phosphatase and tensin homolog (PTEN)-phosphoinositide 3 kinase (PI3K) pathway and Rac1-mitogen activated protein kinase (MAPK) pathway [4,6]. The use of small agents that target these pathways is considered a potential strategy in PCa treatment. NSC23766, a widely used specific inhibitor of the Rac1 pathway, was found to inhibit the progression of PCa in our previous study [7,8]. Nevertheless, understanding how to increase the bioavailability of NSC23766 in PCa treatment remains a problem for NSC23766 use in the clinical treatment of PCa.

Nanotechnologies are widely used in biomedical research and in clinical diagnostics and treatments [9,10]. Several antitumor small agents can be carried to the site by using different nanoparticle delivery systems, such as polyphenol scaffolds [11], polydopamine-based smart materials [12,13] and pH-responsivepolyioncomplexmicelle [14] to reduce toxic side effects and improve bioavailability [9].

In the present study, to prepare the delivery systems, the L-phenylalanine-based poly(ester amide) polymers (8P6 NPs) was synthesized by monomers I and II, which is the carrier of NSC23766. (Figs. S1 and S2 in Supporting information). The particle size of NSC23766@8P6 NPs was 162.3 ± 6.7 nm. The NSC23766 loading capacity was 8.0% ± 1.1% (Figs. 1A and B). TEM measure-

* Corresponding authors at: Department of Urology, Sun Yat-sen Memorial Hospital, Sun Yat-sen University, Guangzhou 510220, China.
** Corresponding author.
E-mail addresses: zhudingjun@163.com (D. Zhu), wujun29@mail.sysu.edu.cn (J. Wu), huangh9@mail.sysu.edu.cn (H. Huang).
[1] These authors contributed equally to this work.

https://doi.org/10.1016/j.cclet.2021.11.078
1001-8417/

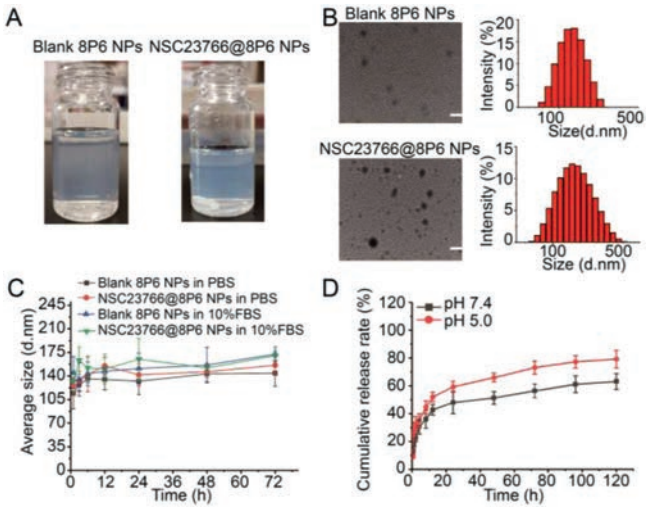

Fig. 1. NSC23766@8P6 NPs are characterized by small particle size and considerable stability. (A) Macroscopic characteristics of the prepared 8P6 NPs. (B) Representative TEM images of blank 8P6 NPs and NSC23766@8P6 NPs (left panels). The particle size of 8P6 NPs and NSC23766@8P6 NPs. (C) Stability characterization of blank 8P6 NPs and NSC23766@8P6 NPs in PBS with and without 10% fetal calf serum for 72 h. (D) The cumulative drug release profiles of NSC23766@8P6 NPs at pH 7.4 and 5.0. Scale bars: 100 nm.

ments indicated that 8P6 NP loading with NSC23766 had similar spherical morphology with slightly increased the particle size. To evaluate the stability of 8P6 NPs, 8P6 NP loading with or without NSC23766 dispersed in PBS (pH 7.4) or 10% FBS solutions was consecutively measured by DLS for 72 h. As shown in Fig. 1C, the 8P6 NPs exhibited excellent stability during the test period. These results demonstrate that 8P6 NPs have an appropriate particle size, a well-defined structure, high NSC23766 loading, and considerable stability in neutral environments.

To measure the release behavior of NSC23766@8P6, *in vitro* drug release assays were performed in PBS and pH 5.0 buffer solution. The results showed that 48.12% ± 7.99% and 59.37% ± 3.89% of NSC23766 was rapidly released from NSC23766–8P6 NPs within 24 h at pH 7.4 and 5.0, respectively, and the final cumulative release at 120 h reached 63.15% ± 5.68% and 79.3% ± 6.34%, respectively (Fig. 1D). It could be proposed that a low pH environment facilitated the rapid release of encapsulated drugs from the 8P6 NPs, which might be beneficial for delivering antitumor drugs to the tumor site with low pH.

To further investigate the cellular distribution and uptake kinetics of NSC23766@8P6, a cellular uptake assay was performed and detected by CLSM. Endolysosomes and NSC23766@8P6 NPs was marked by green and red fluorescence separately, and yellow fluorescence revealed the colocalization of NPs within the endolysosomes. The results also demonstrated that in the PC3 cell line, NSC23766@8P6 NPs colocalized with endosomes within 1 h and were found in the cytoplasm, suggesting rapid cellular uptake kinetics for 8P6 NPs. In addition, cellular uptake level was measured by flow cytometry and confocal laser scanning microscope. (Figs. 2C–E). Coumarin-6 labeled NPs were co-incubated with tumor cells for 4 h. This is accompanied by a rapid increase of the mean fluorescence intensity (MFI) in the first 2 h and a slow rise thereafter, suggesting that 8P6 NPs have dramatic uptake kinetics.

To evaluate the cytotoxic effect of NSC23766 with and without 8P6 NPs, cytotoxicity assays, proliferation assays, and cell cycle analyses were performed to determine the therapeutic effect in PC3 and DU145 cell lines. The results of the cytotoxic effect showed that cell viability decreased rapidly while the concentration of NSC23766 increased from 0 to 100 μmol/L, which was particularly observed in the NSC23766@8P6 NP group. Furthermore, the IC50 values of NSC23766 and NSC23766@8P6 NPs after incubation in DU145 for 48 h were 252.59 μmol/L and 89.16 μmol/L, respectively (Fig. 2A). The IC50values in the PC3 cell line were 46.42 μmol/L and 35.33 μmol/L, respectively (Fig. 2B).

Moreover, the proliferation activity of PCa cells was suppressed more in the NSC23766@8P6 NP group than in the NSC23766 group (Figs. 3A and B, Figs. S3A and B in Supporting information). To further investigate how the nanoparticle system inhibited the proliferation activity of PCa, we conducted cell cycle analysis by flow cytometry (FCM). As shown in Figs. 3C and D, the cell cycle was arrested in the G2/M phase after incubation with NSC23766 or NSC23766@8P6 NPs. The rates of G2/M phase in the NSC23766 and NSC23766@8P6 NP groups increased to 16.04% and 22.30% (in the DU145 cell line) and 10.89% and 18.66% (in the PC3 cell line), respectively. Additionally, migration assays revealed that NSC23766@8P6 NPs reduced the migration cell numbers more effectively than NSC23766 (Figs. S3C and D in Supporting information). These data indicate that 8P6 NPs loaded with NSC23766 suppresses the proliferation and migration of PCa cells more effectively and has a lower IC50 value than NSC23766 alone. The biodistribution and stability of 8P6 NPs in blood circulation is a crucial factor for the bioavailability and therapeutic efficacy of nanoparticle materials [15,16]. The blood compatibility experiment demonstrated that the hemolysis induced by the 8P6 NPs remained lower than 5%, which indicated that 8P6 NPs have good hemocompatibility (Figs. S4A and B in Supporting information). In fact, it is difficult to deliver the drug into tumor tissue specifically by using NSC23766 alone. To verify whether the 8P6 NPs have tumor-targeting characteristics, DiR-labeled 8P6 NPs or DiR alone was injected into mice by intravenous injection and all *in vivo* experiments on mice were reviewed and approved by the ethics boards and the Clinical Research Committee at Sun Yat-sen University. IVIS imaging systems were used to analyze the biodistribution of 8P6 at different time points. As shown in Fig. 4A, DiR was mainly enriched in the liver and spleen but not tumor tissue, while DiR-8P6 NPs gradually concentrated into tumor tissue over time and maintained a high fluorescence signal level at tumor sites after 48 h. These experiments shown that 8P6 NPs possess long blood circulation and passive tumor-targeting ability with desirable hemocompatibility, which is beneficial for improving the antitumor efficacy and decreasing the side effects of small agents *in vivo*.

To explore the antitumor efficacy of NSC23766@8P6 NPs. Normal saline, free NSC23766, 8P6 NPs, or NSC23766@8P6 NPs were intravenously injected into PC3-bearing mice every two days beginning on day 8. Compared with the control and 8P6 NPs group, the tumor growth suppressed by treating with NSC23766@8P6 NP, which behaved a more obviously suppression effect in tumor growth than NSC23766 treated alone (Figs. 4B–D). Moreover, pathology analysis of the tumor tissues was performed to further confirm the therapeutic efficacy of NSC23766@8P6 NPs. Similarly, the NSC23766@8P6 NP group exhibited the lowest expression of the proliferation marker Ki67 and a much higher rate of apoptotic markers cleaved-caspase3 than the other groups (Fig. S5A in Supporting information). It indicated that, after treating with NSC23766@8P6 NP, the proliferation capacity of mice-bearing tumor is much weaker than NSC23766 treated alone while the apoptotic rate is much higher. These results demonstrate that 8P6 NP loading enhanced the antitumor effect of NSC23766 *in vivo*.

In addition to therapeutic efficacy, biosafety is also a very important evaluation index of nanoparticle carriers and small agents. The major organs and blood samples were collected for pathological examination at the end of the study. The H&E staining results revealed that there were no significant changes in the heart, liver, spleen, lung, or kidney among the groups (Fig. S5B in Supporting information). Moreover, blood samples were collected to analyze

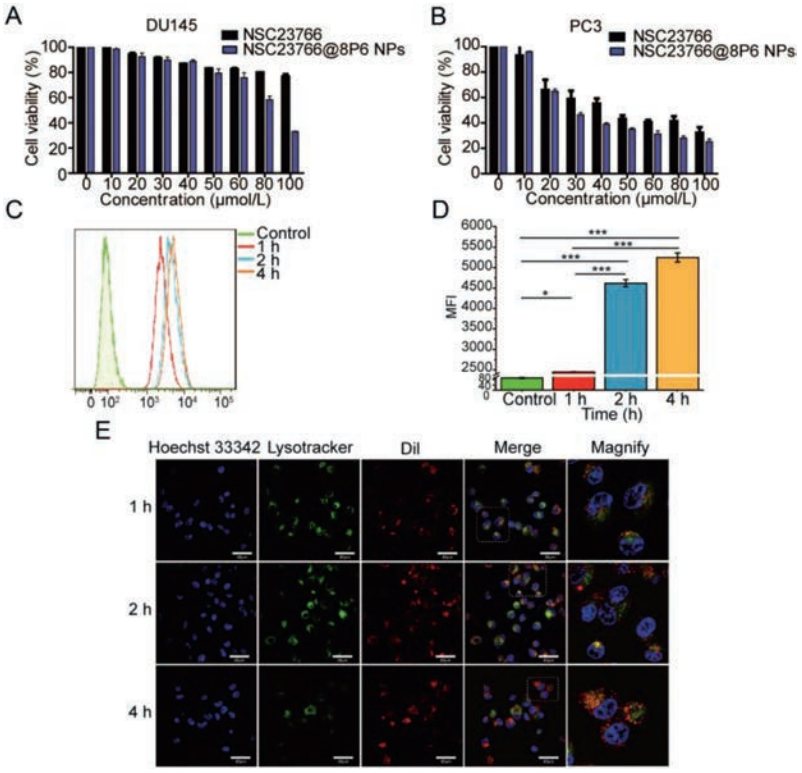

Fig. 2. NSC23766@8P6 NPs exhibit more cumulative drug release at low pH with rapid uptake kinetics. (A and B) Cell viability was measured in DU145 (A) and PC3 cells (B) after incubation with different concentrations of NSC23766 alone or NSC23766@8P6 NPs for 48 h. (C and D) Representative image of cellular uptake analysis by flow cytometry of PC3 cells after incubation with NSC23766@8P6 NPs for 1, 2, and 4 h (D) and quantification analysis of the mean fluorescence intensity. (E) Representative confocal laser scanning microscope images of PC3 cells incubated with DiI-8P6 NPs. The nuclei and endosome were stained with Hoechst 33342 (blue) and LysoTracker green (green), respectively. $^{*}P < 0.05$, $^{***}P < 0.001$. Scale bars: 40 μm (white).

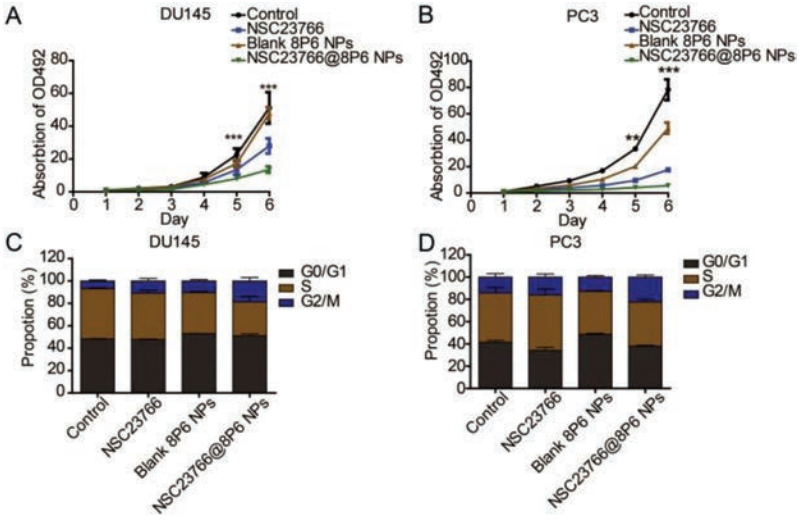

Fig. 3. The 8P6 NP delivery system enhances the cytotoxic effect of NSC23766 *in vitro*. (A and B) Cell viability was evaluated in DU145 (A) and PC3 cells (B) treated with NSC23766 alone or NSC23766@8P6 NPs. (C and D) Flow cytometry analysis of DU145 (C) and PC3 cells (D) treated with NSC23766 alone or NSC23766@8P6 NPs. The percentages (%) of cell populations at different stages of the cell cycle are listed in the panels. $^{**}P < 0.01$, $^{***}P < 0.001$.

the function of the liver and kidney. As shown in Fig. S5C (Supporting information), the indexes of alanine aminotransferase (ALT), aspartate transaminase (AST), blood urea nitrogen (BUN), and creatinine (CRE) in all samples were within the normal range. Collectively, these findings indicate that 8P6 NPs enhance the therapeutic efficacy of NSC23766 with desirable biosafety.

Nanotechnologies have served as a tool for drug delivery systems. The challenges of conventional cancer therapeutic drugs, including nonspecific enrichment, lack of tumor-targeted capability, and low therapeutic efficacy, can be solved by constructing nanoparticle carriers [17–19]. In the past decades, an increasing number of therapeutic products developed from nanomedicine (the application of nanotechnologies to biomedicine) for PCa treatment have entered clinical trials. Bicalutamide, docetaxel, or other agents loaded in liposomal, magnetic, and hybrid nanoparticles decrease systemic cytotoxicity and delay or overcome the development of resistance [9,20–22]. Otherwise, the nanocarrier delivery system played an important role in increasing the effi-

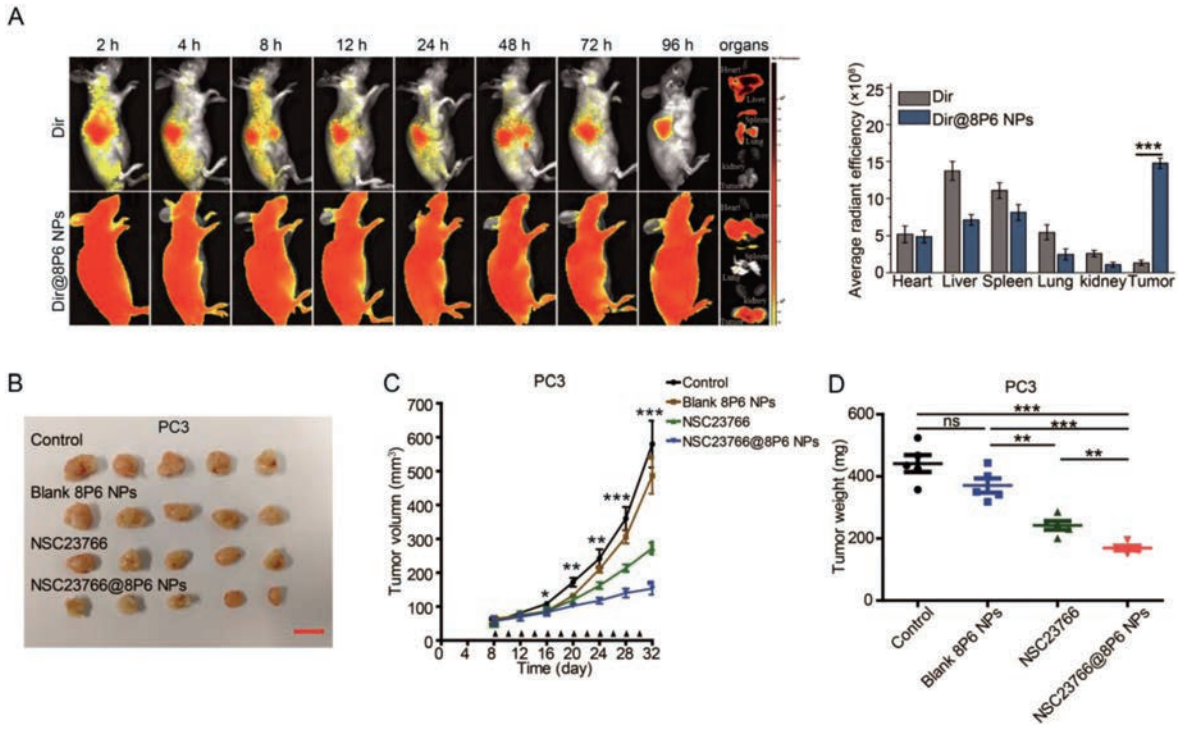

Fig. 4. NSC23766@8P6 NPs are enriched in tumor tissue and enhance therapeutic efficacy against PCa xenografts. (A) *In vivo* biodistribution of DiR and DiR@8P6 NPs in PC3 tumor-bearing mice after intravenous injection for 2, 4, 8, 12, 24, 48, 72, and 96 h and fluorescence images of primary organs and tumors extracted from mice at 96 h (left panels). Quantitative analysis of the fluorescent signals from the major organs and tumors (right panels). (B) Images of tumors excised from mice in the normal saline (control)-, 8P6 NP-, NSC23766 (2.5 mg/kg)- and NSC23766@8P6 NP (NSC23766 dose: 2.5 mg/kg)-treated groups. (C) Tumor growth curves of the four groups. The tumor volume was calculated as the mean ± SD of five mice. (D) Quantitative analysis of the tumor weight from each group. ns: not significant, $^{*}P < 0.05$, $^{**}P < 0.01$, and $^{***}P < 0.001$. Scale bars: 16 mm.

cacy of chemotherapy and immunotherapy [23–25]. The nanoparticles used in this study were fabricated from L-phenylalanine-based polymeric materials, which forming the 8P6 NPs carrier with proper size and structure via hydrophobic forces [26]. The 8P6 NPs delivery systems also behaved long blood circulation, passive tumor-targeting ability, and desirable hemocompatibility, which make the nanoparticles improve the therapeutic efficacy of NSC23766.

NSC23766 inhibits the activation of Rac1 by disrupting the binding between Rac1 and its specific GEFs [7]. Several studies have revealed that NSC23766 plays an effective role in cancer therapy, such as ovarian cancer, breast cancer, and renal carcinoma [27–29]. In our previous study, we found that NSC23766 is a potential therapeutic agent for DEPDC1B-overexpressing PCa patients [8]. To improve the therapeutic efficacy and decrease the concentration of NSC23766 used in treatment, we packaged NSC23766 into 8P6 NPs. Surprisingly, we found that NSC23766@NPs had potent cytotoxicity for PCa with a lower IC50 value than NSC23766 alone *in vitro* and *in vivo*. For further investigation, we determined that NSC23766 arrests the cell cycle in the G2/M phase. Moreover, NSC23766@8P6 NPs did not attack other organs due to the passive accumulation capability of 8P6 NPs.

In summary, NSC23766-loaded Phe-PEA polymer NPs with persistent blood circulation, passive tumor-targeting ability, and desirable hemocompatibility were synthesized by amino acid-based Phe-PEA polymers. NSC23766-8P6 NPs displayed high loading capacity with a low burst effect and optimal drug release *in vitro*. NSC23766@8P6 NPs showed great cytotoxicity in PCa cell lines and xenografts with lower IC50 values and less systemic cytotoxicity. Collectively, NSC23766-8P6 NPs could be promising as a novel strategy in the fight against PCa.

Declaration of competing interest

The authors declare that they have no known competing financial interests or personal relationships that could have appeared to influence the work reported in this paper.

Acknowledgments

This work was supported by the National Natural Science Foundation of China (Nos. 81672550, 81974395); Guangdong Basic and Applied Basic Research Foundation (No. 2019A1515011437); International Science and Technology Cooperation Project Plan of Guangdong Province (No. 2021A0505030085); Sun Yat-sen University Clinical Research 5010 Program (No. 2019005); Sun Yat-sen Clinical Research Cultivating Program (No. 201702); Guangdong Province Key Laboratory of Malignant Tumor Epigenetics and Gene Regulation (No. 2020B1212060018OF006); Guangdong Provincial Clinical Research Center for Urological Diseases (No. 2020B1111170006) to Hai Huang, the National Natural Science Foundation of China (No. 51973243), Fundamental Research Funds for the Central Universities (No. 191gzd35), International Cooperation and Exchange of the National Natural Science Foundation of China (No. 51820105004), Shenzhen Basic Research Project (No. JCYJ20190807155801657), the Project for Science & Technology New Star of Zhujiang in Guangzhou City (No. 201906010082).

Supplementary materials

Supplementary material associated with this article can be found, in the online version, at doi:10.1016/j.cclet.2021.11.078.

References

[1] F. Bray, J. Ferlay, I. Soerjomataram, et al. , CA Cancer J. Clin. 68 (2018) 394–424.
[2] G. Attard, C. Parker, R.A. Eeles, et al., Lancet 387 (2016) 70–82.
[3] M.S. Litwin, H.J. Tan, JAMA 317 (2017) 2532–2542.
[4] T.A. Yap, A.D. Smith, R. Ferraldeschi, et al., Nat. Rev. Drug Discov. 15 (2016) 699–718.
[5] P. Gu, X. Chen, R. Xie, et al., Mol. Cancer 18 (2019) 1–14.
[6] S.M. Kim, T.T. Nguyen, A. Ravi, et al., Cancer Discov. 8 (2018) 866–883.
[7] M. Levay, K.A. Krobert, K. Wittig, et al., J. Pharmacol. Exp. Ther. 347 (2013) 69–79.
[8] Z. Li, Q. Wang, S. Peng, et al., Clin. Transl. Med. 10 (2020) e191.
[9] J. Zhang, L. Wang, X. You, et al., Curr. Top. Med. Chem. 19 (2019) 57–73.
[10] C. Zheng, M. Li, J. Ding, BIO. Integr. 2 (2021) 57–60.
[11] X. Zhang, Z. Li, P. Yang, et al., Mater. Horiz. 8 (2021) 145–167.
[12] P. Yang, F. Zhu, Z. Zhang, et al., Chem. Soc. Rev. 50 (2021) 8319–8343.
[13] J. Hu, L. Yang, P. Yang, et al., Biomater. Sci. 8 (2020) 4940–4950.
[14] P. Zheng, Y. Liu, J. Chen, et al., Chin. Chem. Lett. 31 (2020) 1178–1182.
[15] F. Xiong, X. Ling, X. Chen, et al., Nano Lett. 19 (2019) 3256–3266.
[16] M. Li, X. Zhou, X. Zeng, et al., J. Mater. Chem. B 4 (2016) 547–556.
[17] E. Pérez-Herrero, A. Fernández-Medarde, Eur. J. Pharm. Biopharm. 93 (2015) 52–79.
[18] T. Sun, Y.S. Zhang, B. Pang, et al., Angew. Chem. Int. Ed. 53 (2014) 12320–12364.
[19] X. Feng, W. Xu, X. Xu, et al., Sci. China Chem. 64 (2021) 293–301.
[20] J. Chen, Z. Jiang, W. Xu, et al., Nano Lett. 20 (2020) 6191–6198.
[21] J. Xie, Y. Lu, B. Yu, et al. , Chin. Chem. Lett. 31 (2020) 1173–1177.
[22] C. Xian, Q. Yuan, Z. Bao, et al., Chin. Chem. Lett. 31 (2020) 19–27.
[23] X. Feng, W. Xu, J. Liu, et al., Sci. Bull. 66 (2021) 362–373.
[24] X. Feng, W. Xu, X. Xu, et al., Sci. China Chem. 64 (2021) 293–301.
[25] P. Yu, X. Li, G. Cheng, Chin. Chem. Lett. 32 (2021) 2127–2138.
[26] X. Chen, L. Zhao, Y. Kang, et al., Front. Pharmacol. 9 (2018) 118.
[27] Y. Zhao, Z. Wang, Y. Jiang, et al., Cancer Lett. 313 (2011) 54–63.
[28] Y. Guo, S.R. Kenney, C.Y. Muller, et al., Mol. Cancer Ther. 14 (2015) 2215–2227.
[29] Y.Y. Hsieh, T.P. Liu, P.M. Yang, Pathol. Res. Pract. 215 (2019) 152373.